International Journal of Hydrogen Energy 83 (2024) 589–603

Contents lists available at ScienceDirect

International Journal of Hydrogen Energy

journal homepage: www.elsevier.com/locate/he

Hydrogen production from aluminum reaction with NaOH/H_2O solution: Experiments and insight into reaction kinetics

Veronica Testa [a], Matteo Gerardi [b], Luca Zannini [a], Marcello Romagnoli [a,c], Paolo E. Santangelo [b,c,*]

[a] Dipartimento di Ingegneria "Enzo Ferrari", Università degli Studi di Modena e Reggio Emilia, Modena, Italy
[b] Dipartimento di Scienze e Metodi dell'Ingegneria, Università degli Studi di Modena e Reggio Emilia, Reggio Emilia, Italy
[c] Centro Interdipartimentale di Ricerca e per i Servizi nel Settore della Produzione, Stoccaggio e Utilizzo dell'Idrogeno H2 – MO.RE., Università degli Studi di Modena e Reggio Emilia, Modena, Italy

ARTICLE INFO

Handling Editor: Jinlong Gong

Keywords:
Exothermic reaction
Dietrich-frühling method
Subzero experiments
Active surface
Concentration
Reaction rate

ABSTRACT

Hydrogen as a clean energy carrier is a promising candidate for a shift from fossil fuels to renewable sources. Since hydrogen shall be separated from other elements, various chemical processes may be exploited to this end, including the reaction between aluminum and alkaline solutions. The chemical kinetics of the reaction between aluminum and NaOH/water solution was investigated experimentally in a setup relying on the Dietrich-Frühling method. The parametric analysis encompassed aluminum surface area available for interaction, NaOH concentration and operating temperature, including subzero conditions. Hydrogen production aligned with that predicted through stoichiometric calculations. Moreover, it was demonstrated that reaction rate increases with temperature, concentration and specific surface area of the aluminum samples, also showing how an increase in one of those parameters counterbalances the effect by decreasing another. Finally, activation energy was calculated for the involved reaction as equal to about 50 kJ mol^{-1}, together with Arrhenius coefficient (20526 s^{-1}).

1. Introduction

In the current socioeconomic context, achieving sustainable energy conversion, which implies limited consumption of raw materials and reduced pollution, is one of the most relevant challenges. Notably, the constant population growth – the global population is now over three times larger than it was in the mid-twentieth century [1] and it is estimated that it could increase up to 9.7 billion by 2050 – results in a significant impact on the energy demand to meet the needs of both people and industry [2]. The response to this demand has mainly relied on fossil fuels (e.g., coal, oil, natural gas), the use of which yields negative consequences on atmospheric pollution, greenhouse gas emissions and climate change [3], together with them being finite and depleting resources [1]. So, many research efforts are focused on the study and development of innovative solutions capable of harnessing energy sources and carriers as clean and efficient as possible. In this framework, hydrogen has recently become one of the most promising energy carriers to implement alternative and environment-friendly strategies [4,5]. The transformative shift towards hydrogen-based technologies not only yields reduction of carbon emissions, thanks to water being the only product of its redox reaction with oxygen, but also enhances overall energy efficiency, which ultimately leads to higher sustainability [6]. As an additional advantage, hydrogen stores energy continuously and may transport it wherever it is required [7], unlike other renewable energy sources such as sun or wind, the availability of which is intermittent. Over the last two decades, hydrogen applications have become increasingly widespread, currently encompassing power generation by fuel cells and propulsion by internal combustion engines.

Among the related challenges, hydrogen is a highly flammable element, diffuses into some metals and, above all, its storage and transport may become technically difficult [8]. Storage appears particularly challenging, thus fostering a growing interest in research on methods for continuous and real-time hydrogen production [9], and utilization [10]. As for its production, despite being the most abundant element on Earth, hydrogen is not naturally available as a single H_2 molecule, but can only be found bonded to other elements, such as in

* Corresponding author. Dipartimento di Scienze e Metodi dell'Ingegneria, Università degli Studi di Modena e Reggio Emilia, Padiglione Morselli, Campus San Lazzaro, Via G. Amendola 2, 42122, Reggio Emilia, Italy.
E-mail address: paoloemilio.santangelo@unimore.it (P.E. Santangelo).

https://doi.org/10.1016/j.ijhydene.2024.08.152
Received 11 May 2024; Received in revised form 7 August 2024; Accepted 8 August 2024
Available online 13 August 2024

water and hydrocarbons (e.g., gasoline, methanol and natural gas), predominantly composed of carbon and hydrogen [10]. Hydrogen can be separated through various thermochemical, electrochemical and biological processes. Notably, it can be produced from fossil fuels (i.e., by steam reforming [11], partial oxidation [5] and autothermal reforming or gasification [12]); from water by electrolysis, thermolysis, or photolysis [12] and by microbial fermentation [13] or other chemical processes [14]. Among the last methods, some chemical reactions between metals (e.g., aluminum [15,16], zinc [17], magnesium [18]) and water have been the subject of numerous studies on hydrogen production [15,19].

Notably, the reaction between aluminum and water has been investigated for more than five decades [20–22] as a particularly interesting approach that may benefit from the recycling process of aluminum waste and also from the large availability of liquid water. Aluminum is a highly reactive metal, which implies it can quickly react with water and make gaseous hydrogen separate from the latter. It is also widely available and relatively inexpensive, and safe to handle; the additional products from its reaction with water are non-toxic and can be conveniently disposed of [23]. A Life Cycle Assessment (LCA) study conducted by Hiraki et al. [24] takes both the processes of required deionized water production and residue treatment into account, concluding that the energy requirement for aluminum-based hydrogen production is only 2%v/v and its carbon-dioxide emission is 4%v/v of that generated by conventional production methods (i.e., steam reforming of hydrocarbons). As an additional advantage, aluminum and its alloys appear highly suitable for onboard hydrogen supply in mobile applications, where fuel cells or hydrogen-fueled engines may replace traditional propulsion systems. For instance, a modern FCEV (Fuel Cell Electric Vehicle) available in the market requires approximately 4 kg of hydrogen to cover a running distance of 400 km [25]. This amount of hydrogen can be produced by 36 kg of aluminum through the aluminum/water reaction, assuming 100% conversion yield [26]. Equation (1) expresses the actual reaction between aluminum and water towards hydrogen production [27]:

$$2Al + 6H_2O \rightarrow 2Al(OH)_3 + 3H_2. \quad (1)$$

Despite this reaction is exothermic (i.e., thermodynamically spontaneous), it tends to not occur in the presence of only the involved elements and compounds, since aluminum forms a passivating oxide layer on its outer surface to prevent corrosion. So, several techniques have been developed to facilitate the aluminum/water reaction; among them, the most popular consist of combining oxide (e.g., Al_2O_3) and salt promoters (e.g., NaCl, KCl) [14,23,28] using molten aluminum alloys that include elements as gallium or lithium [29–31] and employing hydroxide promoters (e.g., NaOH, KOH) [31–34]. Notably, adding promoters, such as NaOH and KOH [27], or NaCl [35,36], is instrumental in making the aluminum/water reaction occur by hindering and often preventing the abovementioned formation of an oxide layer. That makes those two techniques particularly attractive in terms of hydrogen yield, which is typically close to or reaches 100% [22]. The overall chemical reaction involving aluminum, water and sodium hydroxide (NaOH) is presented in Eq. (2) [27] and serves as the foundation of the here proposed research, since the reaction between aluminum and a NaOH-based alkaline solution represents the main focus of the present work.:

$$2Al + 6H_2O + 2NaOH \rightarrow 2NaAl(OH)_4 + 3H_2. \quad (2)$$

The exhausted NaOH can be conveniently regenerated through the decomposition of the remaining aluminum hydroxide, which can be recovered and further used in certain water purification treatments, paper production and fire-inhibition systems [24].

The main parameters governing reaction kinetics and hydrogen production rate are reaction temperature (usually identified as the initial aqueous solution temperature), NaOH molar concentration and aluminum morphology, which is practically embodied by the degree of fragmentation of aluminum provided as a reactant [21,22]. As for the last one, aluminum powder has been the subject of numerous works [24,33,34,37–42] with particle size varying between the submicrometric scale and above 400 μm; thin aluminum foils and plates featuring millimetric thickness were also explored [24,27,31,32,37], with remarkable works focusing on recycled aluminum cans [34]. However, it is worth noting that few studies present a comparison between powder and foils or thicker plates [37]. The concentration of the NaOH-based alkaline solution was rarely varied through parametric studies [34] and only at low molarity values (i.e., up to 1 M). On the other hand, the open literature presents results from a relatively wide range of reaction temperature values (i.e., 20–80 °C [21,22]), with several studies including a temperature-based parametric analysis [24,27,34,36–38,40,41]. Remarkably, the research conducted by Yavor et al. [42] shows an extension up to 200 °C reaction temperature, also featuring a wide range (about 180 °C) of tested conditions. Quite interestingly, the activation energy of the aluminum/water reaction evaluated through the available studies presents a non-negligible variability, ranging from about 40 to about 100 kJ mol^{-1} [42–46].

However, a comprehensive and quantitative analysis of reaction rate over a temperature range including subzero conditions does not appear in the current literature, which primarily motivated the present study. Notably, only Liu et al. [47] performed tests on hydrogen yield and reaction kinetics down to −30 °C. Their seminal work served as an inspirational foundation for the here involved experiments; however, they focused on an Al/Li alloy, which makes the present effort unprecedented, as it is referred to pure aluminum reacting with water within an alkaline solution containing sodium hydroxide. A relatively wide temperature range (about 60 °C) was applied towards assessing the effectiveness of the reaction in terms of hydrogen production, energy efficiency and reaction rate, thus also exceeding the range explored in other recognized studies (40–80 °C [27,36]). In the frame of evaluating reaction kinetics, both aluminum powder and foils were employed in the present work, which responds to the previously mentioned demand for more comparative studies. Moreover, molar concentration of the NaOH/water solution was also varied to expand the range evaluated by Ho and Huang [34]. From an engineering standpoint, the automotive field represents the relevant outlet of the results from the present work, which may be applied towards the development of hydrogen-powered or hydrogen-fueled vehicles. Notably, a quantitative assessment of hydrogen yield and production rate from aluminum/water reaction under subzero conditions, typical of the vehicle startup in cold climates, would be ultimately beneficial to onboard vehicle applications, especially towards combining the involved production method with fuel cells as the propulsion system.

2. Materials and methods

2.1. Chemicals and chemical characterization

Samples of both aluminum powder (particle size ranging from 5 to 23 μm, Fig. 1A) and sheets or foils (10 μm thickness, Fig. 2A) were employed in the experiments to assess reaction kinetics as a function of the surface area available for interaction with NaOH/water solution. The particle size distribution of the feedstock powder was assessed by the laser scattering method (Mastersizer 2000 by *Malvern PANAlytical*), using wet dispersion for particle size measurement (Hydro 2000S dispersion unit by *Malvern PANAlytical*); the sheet thickness was measured by caliber. Both powder and sheets also underwent a preliminary evaluation by the BET (Brunauer – Emmett – Teller) method (Accelerated Surface Area and Porosity System ASAP™ 2020 by *Micromeritics*) to measure specific surface area. The obtained results consisted of 0.91 ± 0.01 $m^2\ g^{-1}$ for powder and 0.63 ± 0.01 $m^2\ g^{-1}$ for sheets, which is consistent with the common assumption of specific surface area growing along with degree of fragmentation. Moreover,

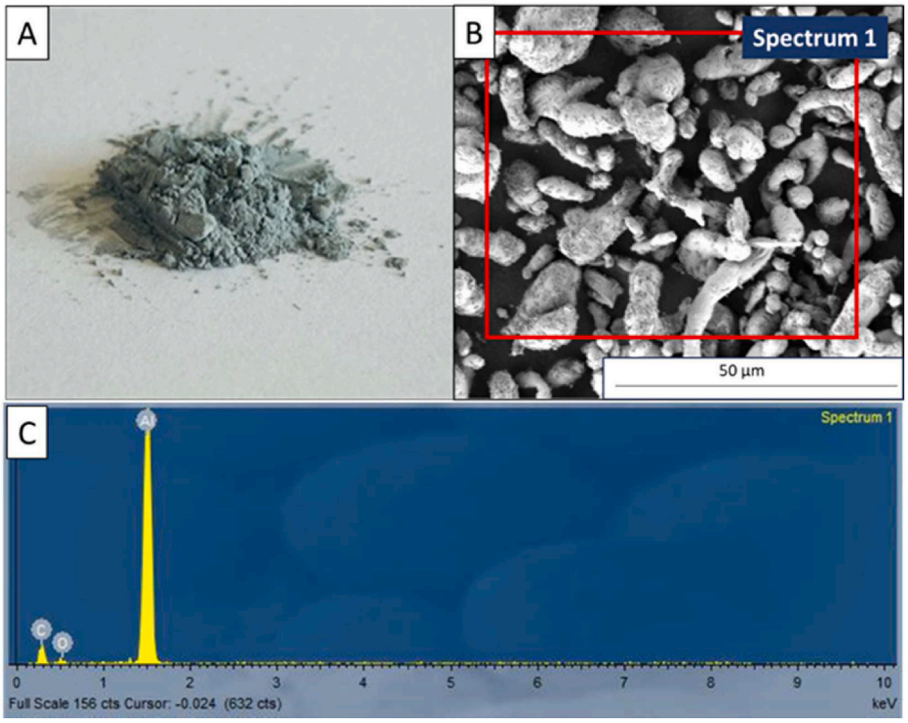

Fig. 1. Sample of the employed aluminum powder: (A) photo; (B) SEM micrograph and (C) EDX spectrum acquired on its top surface.

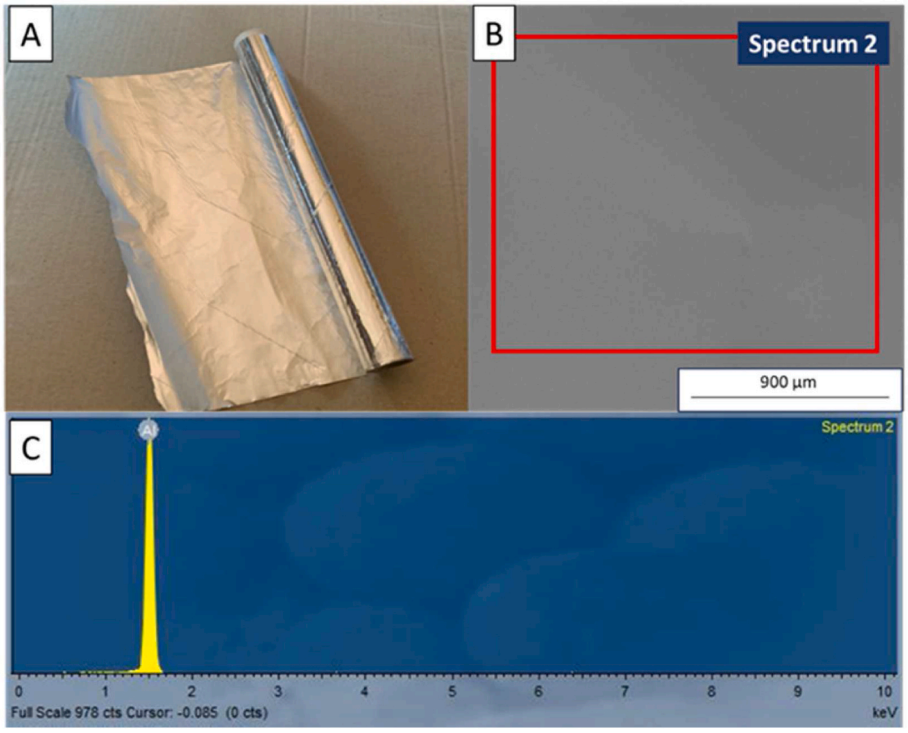

Fig. 2. Sample of the employed aluminum sheets: (A) photo; (B) SEM micrograph and (C) EDX spectrum acquired on its top surface.

powder and sheets were also analyzed by SEM (Scanning Electron Microscopy, Quanta 200 ESEM FEG by *FEI*) to assess their morphology. Some snapshots are presented in Fig. 1B and 2B: the SEM micrographs of powders show irregularly shaped metallic powder with an average size of 10 µm, which appears in accordance with the aforementioned particle-size distribution measurements.

Energy-dispersive X-ray spectroscopy (EDX, Inca Energy 350 Energy Dispersive Microanalysis System by *Oxford Instruments*) and X-ray diffraction (XRD, X'Pert PRO and Empyrean by *Malvern PANAlytical*) were also employed to detect the phase composition of the used aluminum powder and sheets, thus ultimately assessing their purity. The XRD patterns, obtained using Cu-Kα radiation by a tube operated at 40 kV and 40 mA over the $5° < 2\theta < 70°$ range and shown in Fig. 1C and 2C for powder and sheets, respectively, reveal that both can be considered

practically pure (purity greater than 99%). It is worth noting that carbon detected when testing powder (Fig. 1C) belongs to the adhesive tab employed to hold the powder sample; on the other hand, oxygen belongs to ambient air entrapped in the powder. The XRD spectra (Fig. 3) exhibit only aluminum peaks for powder, whereas they also highlight traces of iron and silica together with metallic aluminum in the sheets. However, the EDX spectra acquired on the foils (Fig. 2C) do not show any elements other than aluminum, which allows stating that the concentration of silicon and iron oxides is lower than 1%: the purity of the employed aluminum sheets exceeds 99%. Interestingly, the dominant peaks of aluminum are lower in the sheet sample than in the powder, which is due to the micrometric thickness of the layer of the former, resulting in a weaker signal.

The NaOH/water solution was prepared to test two NaOH molar concentrations: 1 M and 5 M. Notably, NaOH pellets (purity above 98%) were dissolved in distilled water by mechanical stirring.

2.2. Experimental setup

The developed experimental setup implemented the Dietrich-Frühling method, commonly used to assess the amount of gaseous species (e.g., carbon dioxide) rising through a porous solid matrix, as in geodynamics and volcanology [48,49], or to determine the carbonate content of clays [50]. Arguably the first instance of an experiment based on the Dietrich-Frühling method to evaluate hydrogen production from a reaction occurring in a vessel, the employed test rig was aimed at measuring the volume of hydrogen produced by the reaction between aluminum and NaOH within an aqueous solution. The apparatus (Fig. 4) consisted of a metal frame with two vertical parallel rods that held a cylinder graduated from 0 to 200 mL (Fig. 4, item 1), containing liquid water, and another levelling cylinder (Fig. 4, item 2), containing liquid water. The two cylinders were connected by a flexible plastic tube; the graduated cylinder was equipped with a stopcock (Fig. 4, item 3) at its top end, which governed exposure to ambient air for both cylinders; the levelling cylinder was always subject to ambient pressure throughout the experiment, instead. A bottle used as a sample container, a test tube hosting the reactants, a graduated glass beaker for cooling water and a cooling coil are generally inserted as additional components [51]. However, in the present test rig the conventional system was modified to achieve direct reading of the volumetric amount of produced hydrogen on the graduated cylinder. Notably, the small glass channel extending from the bottom end of the graduated cylinder was connected to a bubbler (Fig. 4, item 4) placed in a beaker, by a plastic tube. The bubbler is a common laboratory glassware device used to impose controlled release of gaseous species during a chemical reaction. It appears as a cylindrical bulb with two equally long ends, which can be connected to a vessel where the reaction occurs and to a gas-collecting tank, respectively. In the present apparatus, the bubbler was partially filled with distilled water and connected on one end to the vertical graduated cylinder, thus allowing inflow of the gaseous hydrogen generated by the reaction, and on the other end to a glass flask (Fig. 4, item 5) that contained the NaOH/water solution and aluminum; the flask was sealed before the reaction between aluminum and water occurred.

The purpose of inserting the bubbler was to prevent the presence of any excess water vapor resulting from the reaction within the inflow to the graduated cylinder, by allowing it to bind with the molecules of distilled water hosted in the bubbler itself. This design strategy ensured that the gas inflow into the graduated cylinder only consisted of hydrogen. It is worth clarifying that both the bubbling process and the presence of water in the cylinder did not affect the evaluation of the total amount of produced hydrogen, thanks to the low solubility of hydrogen in water (i.e., from 0.0019 to 0.0011 g per kg of water in the 0–60 °C water temperature range). Once the reaction began, the generated hydrogen passed from the flask to the graduated cylinder, thus increasing the ambient pressure within the cylinder and acting on the liquid water column hosted inside, thus causing its level to decrease and making part of the water flow into the levelling cylinder.

The dependence of reaction kinetics on temperature was assessed as one the scopes of the present work. Notably, the tests were conducted at 25 °C, a condition commonly applied by National Institute of Standards and Technology (NIST) as a standard reference when evaluating the heat exchanged by a reacting system with the surroundings [52], 50 °C and subzero (i.e., −5 to −6 °C) ambient temperature; standard pressure (i.e., 1 bar) was kept as the ambient pressure in all the experiments. In high-temperature tests, the glass flask was placed onto a heating plate to make the temperature of the NaOH/water solution reach 50 °C before starting the reaction by adding aluminum. On the other hand, the experiments conducted below 0 °C featured a mixture of ice and NaCl used

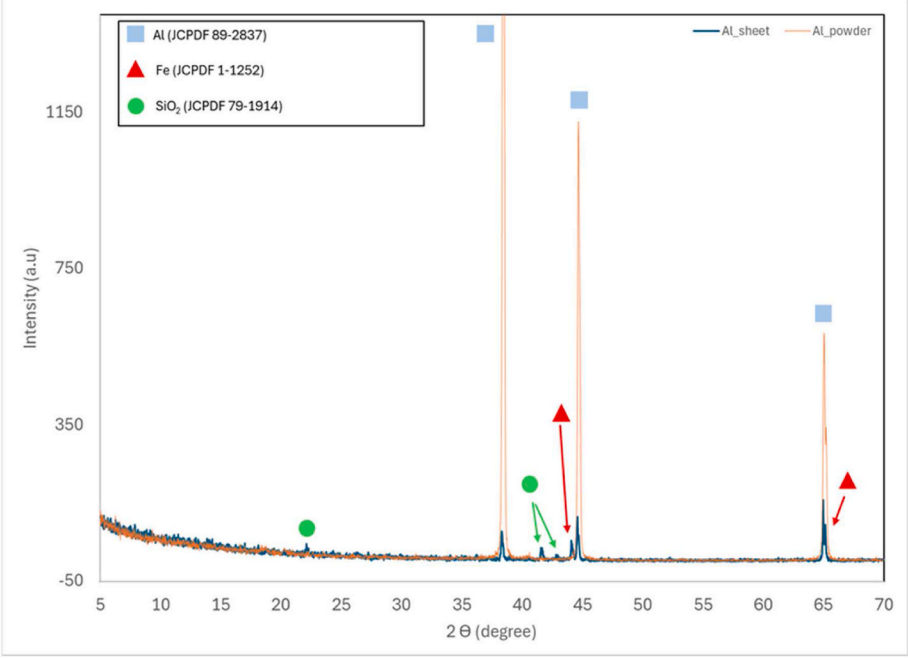

Fig. 3. XRD patterns acquired on samples of the employed aluminum powder and sheets.

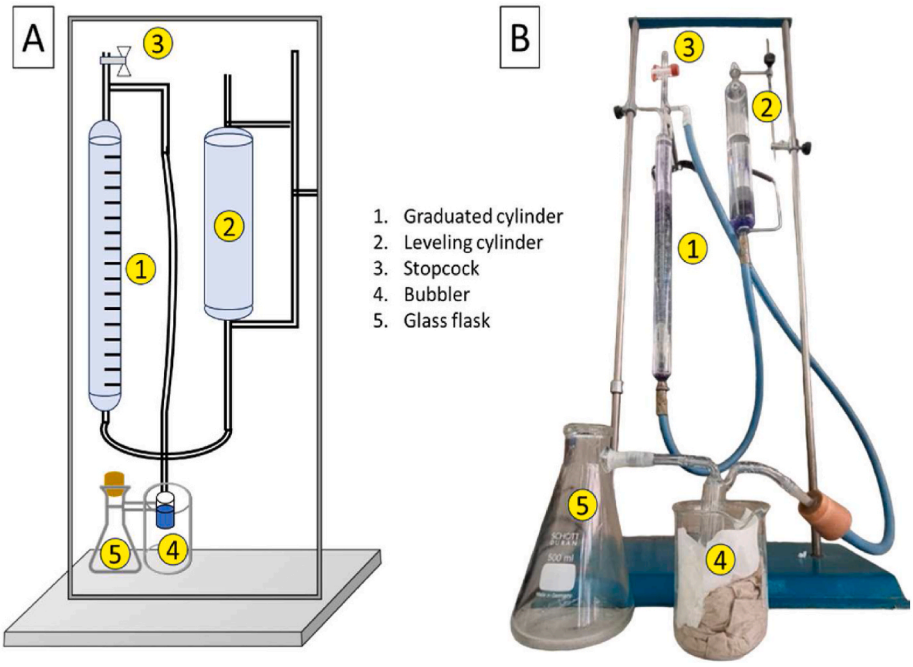

Fig. 4. Experimental apparatus implementing the Dietrich-Frühling method: (A) schematic adapted from Ref. [32] and (B) photo of actual test rig.

as a cooling body for the NaOH/water solution: it was prepared before each of those tests and placed into a container, then the glass flask was inserted into that container before starting the reaction with aluminum. This approach relies on the freezing point depression, one of the colligative properties of solutions: it consists of a drop in the freezing point of a generic solvent, imposed by adding a non-volatile substance (i.e., the solute). The temperature drop can be expressed as $\Delta T = -K_c\, m\, i$, where K_c is the cryoscopic constant of the solvent (1.86 °C kg mol^{-1} for water), m is molality and i is the Van't Hoff factor. The last one can be formulated as $i = 1 + \alpha(\nu - 1)$, where α is the degree of dissociation of the solute (1, as the fraction of dissociated molecules is 100%) and ν is the number of ions generated by dissociation (4, as the reaction produces two Na^+ and two OH^- ions). In the present work, sodium chloride (NaCl, a salt) was mixed with finely chopped ice, thus reducing water freezing point: the process generates a mixture of two solid phases (i.e., ice and salt) and a liquid phase (i.e., the salt dissolved in the small amount of liquid water available in the system); those three phases cannot coexist at temperature above 0 °C, so ice melts until the system reaches the eutectic temperature of −21.3 °C (equilibrium kept throughout complete ice melting or salt dissolution); melting is an endothermic process that requires heat input from the surroundings (i.e., the glass flask containing the NaOH/water solution and aluminum), thereby cooling it down. Ice and sodium chloride initial temperature and mass were assessed to make the NaOH/water solution temperature remain in the −5 to −6 °C range for several hours from start of the reaction. Temperature was measured by a K-type thermocouple inserted within the glass flask (i.e., alkaline solution temperature [21,22]) until the flask was closed upon starting of the reaction. Moreover, temperature was measured at the end of the reaction, resulting in an increase of less than 2 °C with respect to the initial value; that proves the use of a large amount of alkaline solution as an actual heat sink effective in keeping temperature reasonably constant throughout the reaction.

For each tested configuration at standard reference temperature and at 50 °C, seven repeats were conducted to allow performing statistical analysis on the results. On the other hand, six repeats were carried out at subzero temperature and only employing aluminum powder reacting with 5 M alkaline solution; since chemical kinetics is rather slow under that temperature condition, maintaining the desired temperature in the thermodynamic system throughout completion of the reaction proved unfeasible when using aluminum sheets and the lower molar concentration of the NaOH/water solution.

The amount of aluminum to be added for reaction with water was determined to generate a volumetric amount of hydrogen between 70 and 110 mL, a range deemed reasonably aligned with the capability of the described setup, also considering the full scale of the graduated cylinder (200 mL) and the amount of liquid water hosted within at the beginning of each test (200 mL, cylinder fully filled before starting the reaction). The involved chemical reaction requires 2 mol of aluminum for every 3 mol of hydrogen produced, as expressed by Eq. (2); so, the required stoichiometric mass of aluminum as a reactant to achieve the desired volume of hydrogen was calculated, also accounting for temperature dependence of hydrogen density; Table 1 reports the results obtained at −10 and 50 °C solution temperature as representative examples, since they embody the upper and lower bound of the tested range of temperature. Therefore, an aluminum amount equal to 0.060 ± 0.009 g (accuracy of scale included) was employed in the experiments as a conservative value to meet the aforementioned need for not exceeding the maximum volume allowed in the graduated cylinder. Along the same line, the molar mass of the NaOH/water solution required to generate the desired amount of hydrogen was also calculated. The stoichiometric volume of NaOH/water solution required to produce the desired amount of hydrogen was 2 mL. In fact, a significantly higher amount (100 mL) of alkaline solution was used in every test to mitigate the thermal effect of the exothermic reaction (enthalpy of reaction $\Delta H = -277$ to -291 kJ $\text{mol}_{H_2}^{-1}$ in the 0–200 °C temperature range). This approach made the solution an actual heat sink itself, able to uniformly dissipate the generated heat without any significant variation with respect to the initial temperature before starting the reaction, even considering the

Table 1
Stoichiometric amount of aluminum required for the reaction with NaOH/water solution at −10 (lower bound) and 50 °C (upper bound) initial temperature.

Temperature (°C)	Desired H_2 volume (L)	H_2 density (g L^{-1})	Stoichiometric Al moles (mol)	Stoichiometric Al mass (g)
−10	0.70–0.110	0.0922	0.0021–0.0034	0.058–0.091
50	0.70–0.110	0.0736	0.0017–0.0027	0.046–0.072

relatively small volume of the glass flask.

2.3. Experimental procedure and quantitative analysis

Upon pouring the NaOH/water solution into the glass flask and preparing the desired amount of aluminum, the water level into the two cylinders was made the same by adjusting the height of the levelling one. Water was initially subject to ambient pressure in both cylinders; the stopcock on top of the graduated cylinder was closed before starting the reaction to avoid hydrogen outflow and keep the gas within the vessel. The aluminum was either poured (powder) or dropped (sheets) into the glass flask, thus starting the reaction; the glass flask was sealed immediately after the start and kept closed throughout the experiment to convey the produced hydrogen towards the bubbler, without any loss. Each test was videorecorded, thus collecting the history of liquid-water volume hosted in the two cylinders over the course of the reaction.

Once the reaction reached its end, the levelling cylinder was shifted down along the vertical axis to make water height in the two cylinders equal. Subsequently, the stopcock was opened, thus allowing exposure to ambient pressure in both cylinders: the resulting difference between height of water column in the levelling cylinder and that in the graduated cylinder yielded the total volume of produced hydrogen. A procedure was also devised and implemented to reconstruct the actual amount of hydrogen produced through each test as a function of time. It is worth remarking that the volume yielded by the difference read on the graduated scales during the test was biased by ambient pressure acting only on the column of liquid water hosted within the levelling cylinder. Firstly, the hydrostatic law expressed by Eq. (3) was applied to calculate the total pressure $P(t)$ exerted by the air/hydrogen mixture on the liquid column at the generic time t:

$$P(t) = \gamma(h_1 - h_2) + P_{amb}, \tag{3}$$

where P_{amb} is the atmospheric pressure at the beginning of the experiment (i.e., within the cylinder right before starting the reaction), γ is the specific weight of the involved liquid (water, in the present experiment), h_1 and h_2 is the height of the liquid column in the levelling cylinder (right) and in the graduated cylinder (left) at the generic time t, respectively (Fig. 5).

As a commonly acknowledged assumption, hydrogen was considered as an ideal gas; so, Boyle law expressed by Eq. (4) was applied to calculate the actual volumetric amount of hydrogen V at the generic time t:

$$V(t) = \frac{\left(V_f - V_f'\right)\cdot(P(t) - P_{amb})}{P_f' - P_{amb}} + V'(t), \tag{4}$$

where V_f is the total volume of produced hydrogen, V_f' is the final volume of hydrogen read before shifting the levelling cylinder down and corresponding to pressure P_f' calculated by Eq. (3) and $V'(t)$ is the volume of hydrogen read on the videoframes at time t. Overall, the reconstruction procedure consisted of correcting the last parameter.

2.4. Statistical analysis

The whole dataset was also analyzed by statistical methods to check whether statistically different kinetics occurred or not while varying temperature, NaOH concentration within the solution and aluminum degree of fragmentation (i.e., powder and sheets). As the first step of the procedure, normality test was applied against the distribution of data (i.e., produced hydrogen volume) in each condition defined by a set of values for temperature, concentration and degree of fragmentation (i.e., a group). Notably, the Shapiro-Wilk test [53]was employed to the purpose: dating back to 1965, it is a statistical test used to determine whether a sample or a dataset exhibits a normal distribution or not. It is based on the Kendall's W, which evaluates the discrepancy between observed data and the values expected if following normal distribution; W statistic ranges from 0 to 1, with values close to 1 emphasizing good fitting with normal distribution. The Shapiro-Wilk test is recognized for its effectiveness for small to moderate sample sizes and its implementation is rather seamless in most statistical software packages. As a representative parameter, the time required for 90% of the reaction to take place (i.e., the time to reach 90% of the whole hydrogen produced in a single test) was considered to build the dataset for each group. If the data passed the Shapiro-Wilk test for normality and Levene test to check the equality of variances for groups, ANOVA (Analysis of Variance) was then conducted to determine if any statistically significant difference occurred with 95% confidence level among groups. If the Levene test was negative, then the Unequal-variance (Welch) ANOVA was used. If the data do not have a normal distribution according to the Shapiro-Wilks test, then the Kruskal-Wallis test was applied. ANOVA assesses the statistically significant difference – if any – among group means by dividing the total variance into between-group variance and within-group variance [54], thereby checking the Null Hypothesis (i.e., groups of data come from the same population or exhibit the same median). Notably, the two quantities are expressed by Eqs. (5) and (6), respectively:

$$s_b^2 = \sum_{i=1}^{n_j} n_j \left(\overline{x_{ij}} - \overline{X}\right)^2, \tag{5}$$

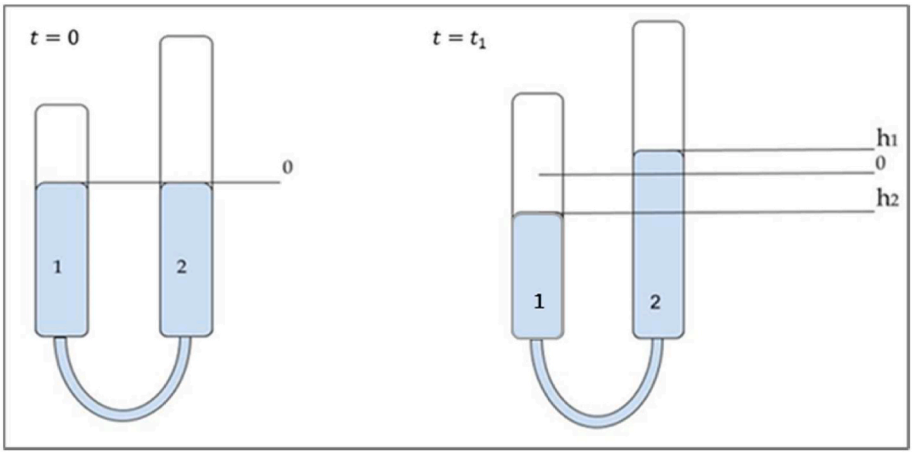

Fig. 5. Schematic of the cylinders in the developed Dietrich-Frühling apparatus; t is time, $t = 0$ represents the starting time of the reaction and t_1 is a generic time during the reaction, *0* is the level of the liquid column before start of the reaction.

$$s_w^2 = \sum_{j=i}^{k} \sum_{i=1}^{n_j} \left(x_{ij} - \overline{x_{ij}}\right)^2, \quad (6)$$

where s is variance, k is the number of groups, n is the number of observations (i.e., data), x_{ij} identifies each observation, $\overline{x_{ij}}$ is the mean value over the single group, $\overline{X}$ is the overall mean of x_{ij}, b and w are indexes referring to between-group and within-group, respectively, i and j are indexes within observations and groups, respectively. The F-value was then calculated by dividing the between-group variance by the within-group variance $\left(\frac{s_b^2}{s_w^2}\right)$, which indicates whether the group means are significantly different. The calculated F-value was finally compared with a F-critical value that depends on the degree of freedom consistent with a selected error level α. *Post hoc* tests, such as Tukey's range test, were also performed to determine which groups differ from each other. On the other hand, the Kruskal-Wallis test [55,56] is another nonparametric statistical test used to compare distributions of two or more independent groups to check the Null Hypothesis. The test is based on the ranks of data, rather than actual values and it does not assume normal distribution or homogeneity of variance, so it is particularly useful when data are not normally distributed, being less sensitive to outliers and deviation from normality than other parametric tests. After the Kruskal-Wallis test, the Dunn's test typically follows as a nonparametric, *post hoc* test not relying on normal distribution or homogeneity of variance. That test is typically used to identify which groups are significantly different from the others and is based on the comparison between mean ranks of the groups. The p-value $(p = 1 - \alpha)$ of Tukey's and Dunn's tests indicates the level of significance and determines if the difference between two groups is statistically significant; it is compared to a chosen significance level (e.g., 0.05) to check whether the Null Hypothesis holds or not: if p-value is lower than the significance level, Null Hypothesis is rejected and the difference between the two investigated groups is deemed statistically significant. All the calculations were performed employing the PAST software [57].

3. Results and discussion

3.1. Experiments at standard reference temperature

As the first and most straightforward experiments conducted by the apparatus described in Section 2, the results from tests at standard reference temperature (25 °C) are presented in Table 2. Notably, it displays the comparison between the stoichiometric hydrogen volume yielded as a product of the reaction and the volume measured for the 1 M alkaline solution.

The results reveal a slight difference between stoichiometric and measured values. The average relative discrepancy is rather low (in the order of 1%), with the maximum discrepancy being lower than 5.5%, and may be due to the systematic measurement error occurring in weighing the aluminum amount used in each experiment (i.e., accuracy of the scale). Additionally, the difference between the two values could be also linked to minimal hydrogen losses due to a slightly less-than-perfect closure of the graduated cylinder by the stopcock (systematic), the reported minimal solubility of hydrogen in water (systematic) and to random error in reading final hydrogen volume. Nevertheless, the discrepancy between the two values appears sufficiently negligible to consider the experiment capable of evaluating the amount of produced hydrogen and to allow considering hydrogen yield virtually equal to 100%, in consistency with other studies where the same reaction is involved [24,27,33,42] and supporting the ability of hydroxide promoters to maximize that parameter [22]. Consequently, the evolution over time of generated hydrogen also appears effectively monitored through the tests conducted under the selected conditions.

Table 2
Hydrogen volume produced at 25 °C by aluminum powder and sheet reacting with 1 M NaOH/water solution: comparison between stoichiometric and measured values.

Conducted test	Al powder		Al sheet	
	Stoichiometric H_2 volume (mL)	Measured H_2 volume (mL)	Stoichiometric H_2 volume (mL)	Measured H_2 volume (mL)
1	83.58	79.00	84.54	84.50
2	84.54	84.30	86.07	87.60
3	85.23	85.00	88.43	88.70
4	86.60	86.60	91.06	90.60
5	89.48	90.00	91.62	92.00
6	92.64	93.00	92.86	92.80
7	95.52	96.10	93.14	93.10

The trends of hydrogen production as a function of time throughout the involved reaction are shown in Fig. 6 and for 1M NaOH/water solution reacting with aluminum powder and sheet, respectively, and in Figs. 8 and 9 for 5 M NaOH/water solution reacting with aluminum powder and sheet, respectively. Hydrogen amount is presented as a volume over mass of aluminum used in each test, thus making the results independent of the actual amount of aluminum employed in each test. The seven curves – seven repeats of the same experiment for each tested configuration – exhibit a consistent profile and practically overlap. In general, and particularly in Fig. 7 the profiles reveal three distinct phases throughout the reaction:

- an initial phase: the reaction has just started and the slope is rather low;
- an acceleration phase: rapid increase in produced hydrogen over time (i.e., steeper slope);
- a final phase: the curve grows at a slower rate, approaching stabilization before the end; reaction rate slows down even further slowed down as the reactants are depleted and the reaction approaches equilibrium (i.e., plateau).

About tests run by the 1 M solution, evidence of the complex nature of the process appears evident in the curves related to aluminum sheets (Fig. 7), where the duration of each test is far more prolonged compared to that related to aluminum powder (Fig. 6). Specifically, the former requires 810 s to reach completion at a 25 °C temperature, while the latter reaches the end in 480 s. This significant difference can be attributed to the higher specific surface area of aluminum powder (Subsection 2.1), which makes a larger surface available for interaction and reaction with water per unit mass. This outcome was also found for aluminum reacting with water [58]. From a phenomenological standpoint, a larger space for particle collision on the reactant surface is thereby available, which promotes higher reaction rate: in the case investigated here, interactions between aluminum and the solution become accelerated, thus expediting the overall reaction. So, in the plot showing the dataset for aluminum powder, the reaction appears to swiftly progress into the acceleration phase, with the initial phase being so rapid that it seems practically instantaneous.

When using a 5 M solution, the found trends remained qualitatively unchanged with respect to the 1 M solution. As expected, the substantial difference between the two tested values of molar concentration lies in the duration of the experiments: indeed, employing a higher concentration means a significantly shorter reaction time. Specifically, the reaction of 5 M NaOH/water solution with aluminum powder reached its end in 110 s (Fig. 8), while that with an aluminum sheet did in 340 s (Fig. 9) at standard reference temperature, which range between 20%–40% the reaction time with 1 M concentration. This outcome is consistent with the formulation proposed in Subsection 2.3 about chemical reaction kinetics: reaction rate grows proportionally to the reactant concentration.

The groups collected at standard reference temperature investigated through statistical analysis (Subsection 2.4) exhibited a normal trend,

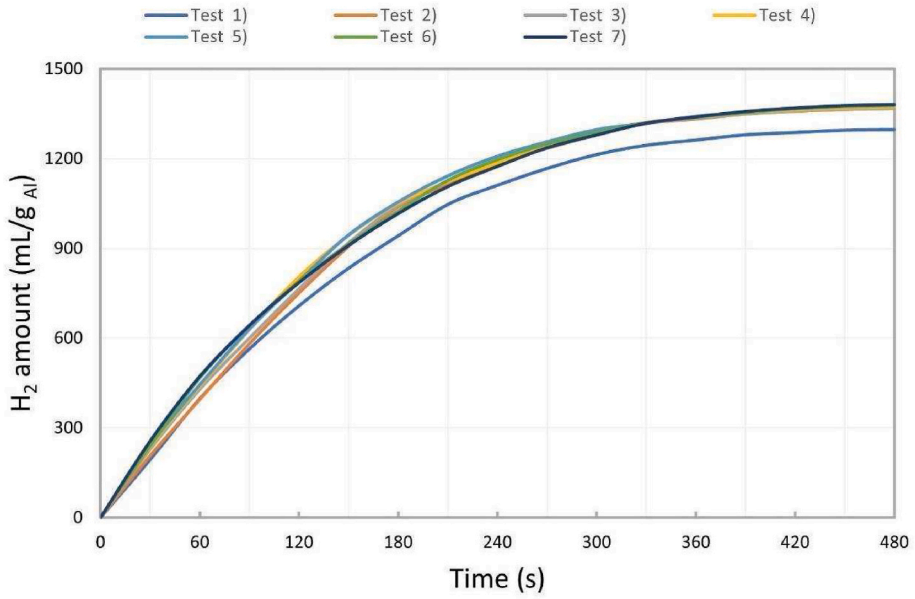

Fig. 6. Aluminum powder reacting with 1 M NaOH aqueous solution: hydrogen produced at room temperature normalized by the amount of employed aluminum, as a function of time (all the seven repeats displayed).

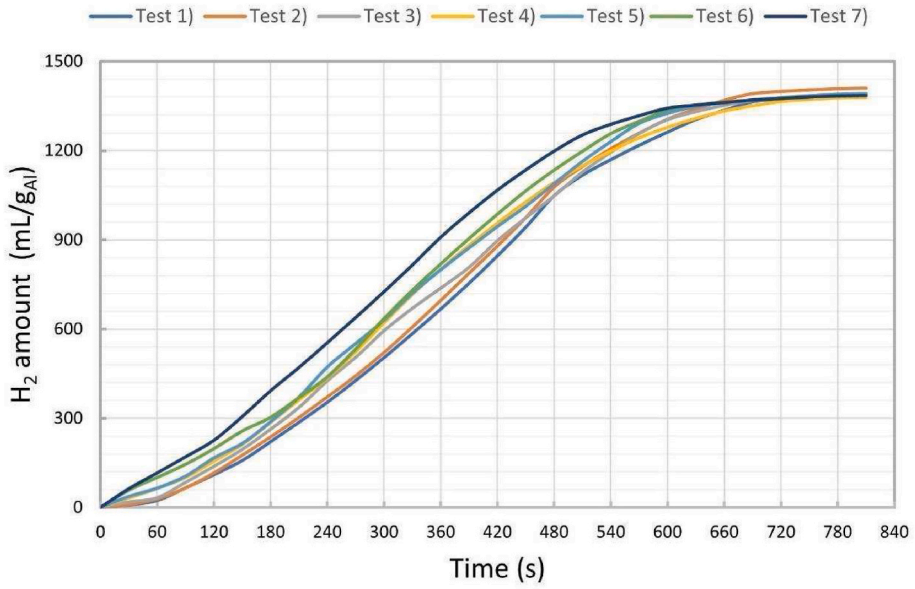

Fig. 7. Aluminum sheets reacting with 1 M NaOH aqueous solution: hydrogen produced at room temperature normalized by the amount of employed aluminum, as a function of time (all the seven repeats displayed).

based on the Shapiro-Wilk test. The samples failed the Levene test for homogeneity of variance; therefore, the unequal-variance (Welch) ANOVA was carried out to determine if any statistically significant difference arose with reference to NaOH concentration and degree of fragmentation of the aluminum samples (i.e., powder or sheets). It was found that the statistical difference occurred with 95% level of significance. Subsequently, Tukey's post hoc test was also performed, which confirmed that all the tested conditions differ from each other in terms of outcomes, which allows claiming that degree of fragmentation of aluminum samples and molarity of the NaOH/water solution impact on reaction kinetics. In the case of aluminum powder, the increase in NaOH concentration makes reaction rate increase by about six times, while a twofold increase occurs in the case of aluminum sheets. Moreover, under the same NaOH concentration, aluminum powder yields faster kinetics, which becomes more evident with 5 M NaOH/water solution. Table 3 reports a summary of statistical parameters resulting from ANOVA and Tukey's *post hoc* test against the dataset collected at 25 °C; reaction time as defined in Subsection 2.3 is included as representative of reaction kinetics.

3.2. Experiments at high temperature

Figs. 10 and 11 show the amount of hydrogen produced at 50 °C with 1 M alkaline solution. Even at the higher temperature, the obtained values correspond to the stoichiometric ones with very low degree of approximation and the seven curves in each plot display a consistent trend. In consistency with Arrhenius equation [59] an increase in temperature implies a decrease in the overall duration of the reaction since

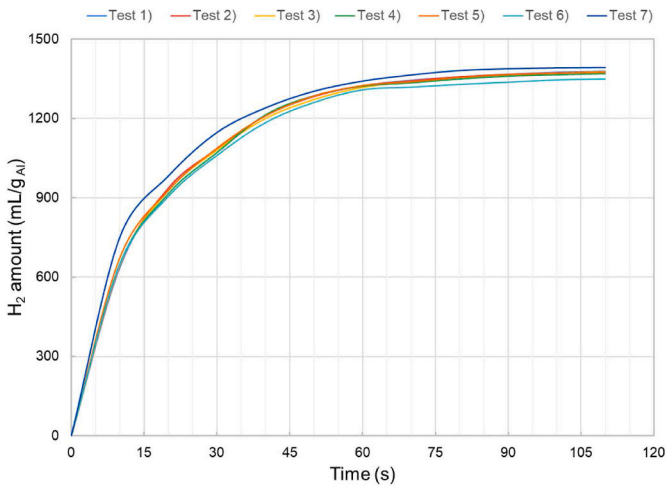

Fig. 8. Aluminum powder reacting with 5 M NaOH aqueous solution: hydrogen produced at room temperature normalized by the amount of employed aluminum, as a function of time (all the seven repeats displayed).

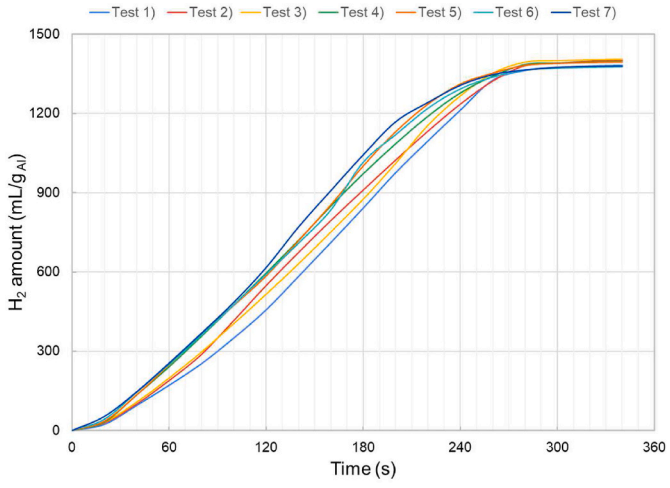

Fig. 9. Aluminum sheets reacting with 5 M NaOH aqueous solution: hydrogen produced at room temperature normalized by the amount of employed aluminum, as a function of time (all the seven repeats displayed).

kinetics becomes faster. For instance, aluminum powder reacting with the alkaline solution reached the end by 45–75 s, while aluminum sheets did the same by 180–240 s. The initial phase of the reaction for aluminum powder was virtually instantaneous and unperceivable, as much as it was for aluminum powder reacting at standard reference temperature; indeed, the curves exhibit strong acceleration from the onset of the reaction (Fig. 10). However, as opposed to what occurred at standard reference temperature, the same behavior also occurred for aluminum foils reacting with the alkaline solution at 50 °C nominal temperature. This phenomenon can be related to temperature as a parameter representing kinetic energy of the involved particles: the higher the temperature, the higher the energy, which allows particles participating in the reaction to quickly overcome activation energy. That reduces the initial phase down to an instantaneous mechanism even when the surface available for interaction per unit mass is lower (i.e., for aluminum foils). The plots of Figs. 12 and 13 support an observation already mentioned about tests at standard reference temperature (Subsection 3.1): increasing the concentration of the solution makes the reaction proceed more rapidly. Specifically, aluminum powder reacting with 5 M alkaline solution reached the end by 14–24 s, while aluminum sheets did by 45–70 s. In an analogous manner to the tests with lower

Table 3
Summary of the statistics related to reaction time at standard reference temperature; the last four lines show the values of Tukey's *post hoc* test.

	Al powder + 1 M	Al sheets + 1 M	Al powder + 5 M	Al Sheets + 5 M
Mean reaction time (s)	267.212	556.26	43.70	233.87
Standard error (s)	1.58	10.63	0.40	3.96
Median (s)	266.79	566.91	43.96	235.27
Variance (s^2)	17.5548	790.8282	1.1458	109.6882
Minimum value (s)	261.44	506.72	42.18	220.10
Maximum value (s)	274.38	589.57	45.46	246.04
Count	7	7	7	7
Confidence level (95.0%)	3.88	26.01	0.99	9.69
Shapiro-Wilk (*p*-value)	0.9536	0.6640	0.5106	0.3368
Levene test on means (*p*-value)	0.0002002			
Unequal-variance (Welch) ANOVA (*p*-value)	$1.716 \bullet 10^{-17}$			
Al powder + 1M (*p*-value)		$1.714 \bullet 10^{-14}$	$1.714 \bullet 10^{-14}$	0.002088
Al sheets + 1M (*p*-value)	$1.714 \bullet 10^{-14}$		$1.714 \bullet 10^{-14}$	$1.714 \bullet 10^{-14}$
Al powder + 5M (*p*-value)	$1.714 \bullet 10^{-14}$	$1.714 \bullet 10^{-14}$		$1.714 \bullet 10^{-14}$
Al Sheets + 5M (*p*-value)	0.002088	$1.714 \bullet 10^{-14}$	$1.714 \bullet 10^{-14}$	

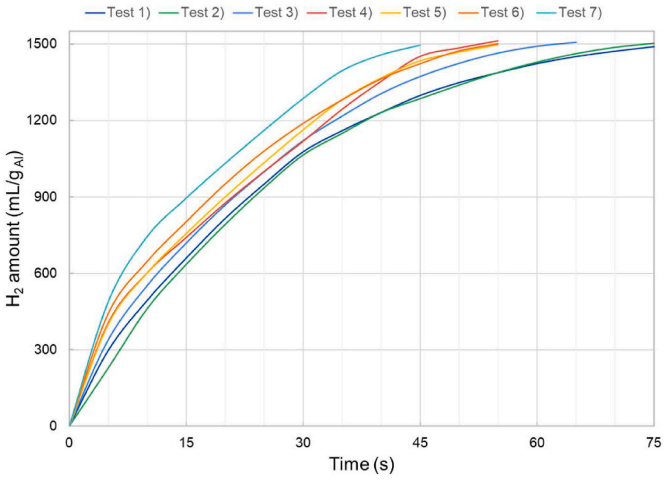

Fig. 10. Aluminum powder reacting with 1 M NaOH aqueous solution: hydrogen produced at 50 °C nominal temperature normalized by the amount of employed aluminum, as a function of time (all the seven repeats displayed).

concentration, the initial phase was also virtually instantaneous, even when aluminum sheets were employed.

As for the dataset collected at standard reference temperature (Subsection 3.1), the difference in terms of reaction kinetics between groups when varying NaOH concentration and degree of fragmentation of aluminum samples was also investigated for the higher temperature value by statistical analysis. The Shapiro-Wilk test showed that not all the groups of data followed a normal distribution; notably, the group obtained by tests with aluminum powder and 5 M NaOH solution did not exhibit a normal distribution. So, the Kruskal-Wallis test was conducted to analyze the whole dataset. Their results proved the groups statistically different, with Dunn's *post hoc* test highlighting a strong, statistically significant (95% level of significance) difference between all groups, except for aluminum powder reacting with 1 M alkaline solution and aluminum sheets reacting with 5 M alkaline solution. Interestingly, this analysis suggests that an increase in NaOH concentration

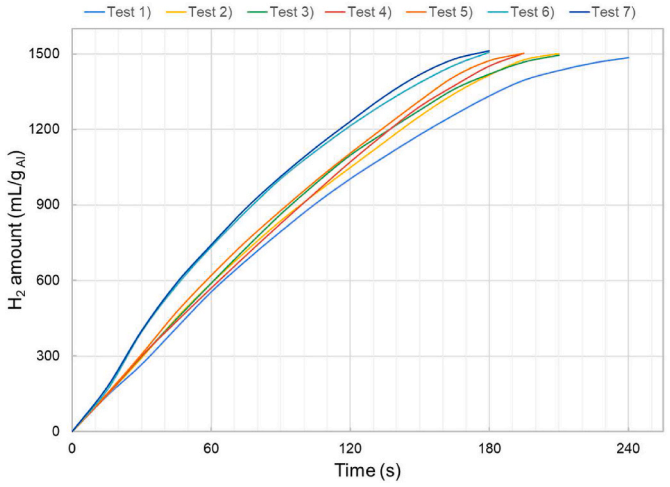

Fig. 11. Aluminum sheets reacting with 1 M NaOH aqueous solution: hydrogen produced at 50 °C nominal temperature normalized by the amount of employed aluminum, as a function of time (all the seven repeats displayed).

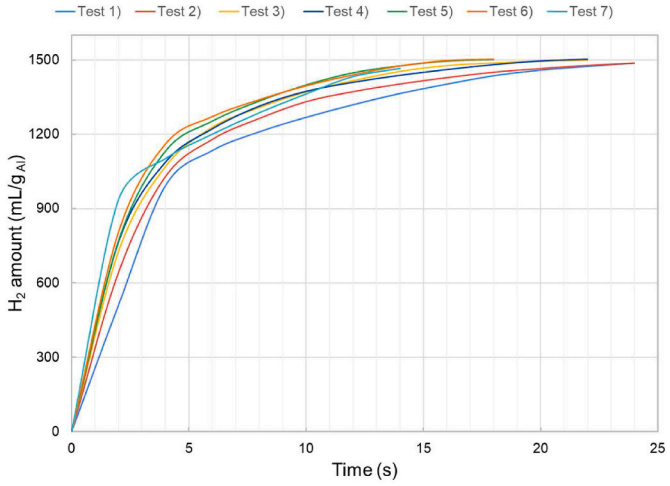

Fig. 12. Aluminum powder reacting with 5 M NaOH aqueous solution: hydrogen produced at 50 °C nominal temperature normalized by the amount of employed aluminum, as a function of time (all the seven repeats displayed).

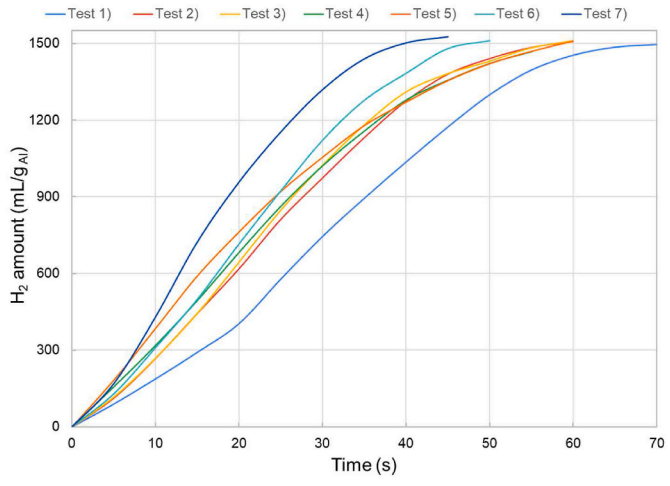

Fig. 13. Aluminum sheets reacting with 5 M NaOH aqueous solution: hydrogen produced at 50 °C nominal temperature normalized by the amount of aluminum employed, as a function of time (all the seven repeats displayed).

counterbalances the effect of a smaller surface available for interaction per unit mass on reaction kinetics, when temperature grows beyond a certain threshold. Even at higher temperature values, the increase in NaOH concentration makes reaction kinetics increase; when keeping NaOH concentration constant, aluminum powder yields faster reaction rate, which becomes more evident with 5 M alkaline solution. These findings appear consistent with those discussed about the dataset obtained at standard reference temperature. Table 4 reports a summary of statistical parameters resulting from Kruskal-Wallis and Dunn's post hoc test against the dataset collected at 50 °C nominal temperature.

3.3. Subzero experiments

As mentioned in Subsection 2.1, the available dataset from subzero tests is limited to aluminum powder reacting with 5 M alkaline solution, due to the slow kinetics at such temperature conditions and difficulty with keeping temperature constant over a lengthy period. Fig. 14 shows hydrogen volume at subzero temperature in the tested configuration: the duration of the reaction is substantially longer compared to tests conducted at standard reference and even higher temperature. This outcome was much expected, as a direct consequence of Arrhenius law (Subsection 2.3) and the dependence of reaction rate on temperature. The slow kinetics at subzero temperature allowed emphasizing the three phases described in Subsection 3.1, with specific reference to the initial phase featuring the lower hydrogen production rate, which appears even more evident than it was for aluminum sheets reacting with 1 M alkaline solution at standard reference temperature (Fig. 7). The three phases could be distinguished by quantifying the change in the slope of each curve of Fig. 14. As mentioned in Subsection 2.2, the experiment under subzero temperature condition was repeated six times.

Usually, if the *p*-value is small ($p < 0.05$), the sample has a distribution significantly different from normal. Based on this assumption, the dataset collected at subzero temperature does not follow a normal distribution. The samples also failed the Levene test for homogeneity of variance. Therefore, the ANOVA test was not performed, due to the absence of normality and homogeneity conditions of the variance and only the Kruskal-Wallis test could be carried out. Table 5 reports a comparison between the statistics related to the subzero tests and the same reactant configuration evaluated at standard reference and 50 °C temperature. According to Dunn's *post hoc* test, there is a significant

Table 4
Summary of the statistics related to reaction time at 50 °C nominal temperature; the last four lines show the values of the Dunn's *post hoc* tests.

	Al powder + 1 M	Al sheets + 1 M	Al powder + 5 M	Al Sheets + 5 M
Mean reaction time (s)	42.25	158.82	9.67	43.00
Standard error (s)	2.44	5.19	0.58	2.35
Median (s)	40.41	161.18	9.31	43.91
Variance (s^2)	41.5574	188.2558	2.3833	38.5486
Minimum value (s)	32.75	140.05	8.47	32.24
Maximum value (s)	51.43	180.91	12.86	52.44
Count	7	7	7	7
Confidence level (95.0%)	5.96	12.69	1.43	5.74
Shapiro-Wilk (*p*-value)	0.7543	0.8645	0.02956	0.6009
Kruskal-Wallis		$4.367 \bullet 10^{-5}$		
Al powder + 1M (*p*-value)		0.01354	0.02107	0.871
Al sheets + 1M (*p*-value)	0.01354		$1.788 \bullet 10^{-6}$	0.02107
Al powder + 5M (*p*-value)	0.02107	$1.788 \bullet 10^{-6}$		0.01354
Al Sheets + 5M (*p*-value)	0.871	0.02107	0.01354	

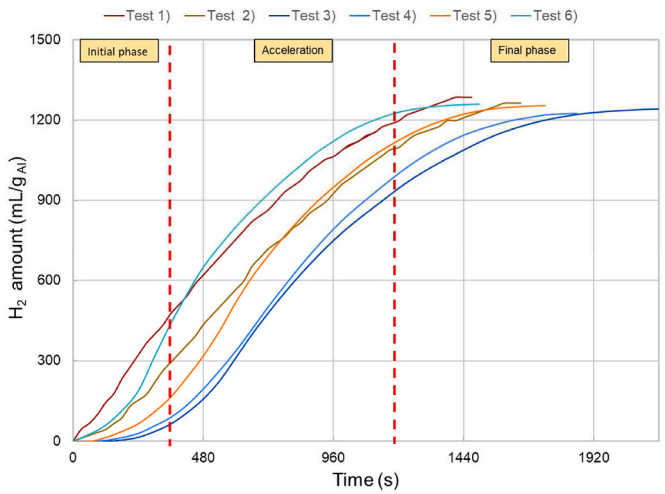

Fig. 14. Aluminum powder reacting with 5 M NaOH aqueous solution: hydrogen produced at subzero (−5 to −6 °C) temperature normalized by the amount of employed aluminum, as a function of time (all the six repeats displayed); the three phases are separated by vertical red lines. (For interpretation of the references to colour in this figure legend, the reader is referred to the Web version of this article.)

Table 5
Summary of the statistics related to reaction time at subzero temperature, with a comparison against the same reactant configuration at the other tested temperature values; the last three lines show the values of the Dunn's *post hoc* tests.

	Aluminum powder + 5 M, subzero	Aluminum powder + 5 M, standard reference temperature	Aluminum powder + 5 M, higher temperature
Mean reaction time (s)	1268.72	43.70	9.67
Standard error (s)	81.98	0.40	0.58
Median (s)	1289.50	43.96	9.31
Variance (s^2)	40321.6300	1.1458	2.3833
Minimum value (s)	970.24	42.18	8.47
Maximum value (s)	1498.33	45.46	12.89
Count	6	7	7
Shapiro-Wilk (*p*-value)	0.8201	0.5106	0.02956
Kruskal-Wallis (*p*-value)		0.0002139	
Aluminum powder + 5M, subzero (*p*-value)		0.04823	$4.103 \bullet 10^{-5}$
Aluminum powder + 5M, standard reference temperature (*p*-value)	0.04823		0.02686
Aluminum powder + 5M, higher temperature (*p*-value)	$4.103 \bullet 10^{-5}$	0.02686	

difference between the tests run at subzero and higher temperature and between standard and higher temperature. On the contrary, there is a lower statistical difference between the tests run at subzero and standard temperature, as shown in Table 5. Overall, decreasing temperature down to below 0 °C strongly impacts on reaction kinetics (i.e., reducing), which is consistent with the theory discussed in Subsection 2.3.

To the same purpose and aiming at a broader comparison, Fig. 15 includes the reaction time as defined in Subsection 2.3 for all the tested configurations. Notably, box plots are shown in the diagram to consolidate all the statistical information related to each group: each box is limited by first and third quartile, also including the median; the whiskers extend from maximum to minimum. Quite interestingly, aluminum powder reacting with 5 M alkaline solution at standard reference temperature exhibits almost the same reaction rate as aluminum powder reacting with 1 M alkaline solution and aluminum sheet reacting with 5 M alkaline solution, both which occurring at the higher temperature (i.e., 50 °C nominal). In consistency with the theory discussed in Subsection 2.3 and as already pointed out in Subsection 3.2, higher temperature somewhat counterbalances the effect of lower concentration and vice versa, while the effect of higher temperature also compensates for that of smaller surface area available for interaction per unit mass. As expected, reaction rate in subzero temperature conditions is remarkably slowed down with respect to any other tested configuration, whereas the fastest occurs when aluminum powder is combined with alkaline solution under the higher concentration, at the higher temperature.

3.4. Discussion and assessment of chemical kinetics

Towards confirming the completion of the investigated reaction with the products included in the reaction of Eq. (2), XRD and EDX analysis were also performed on the anhydrous byproducts at the end of the reaction. The results are here presented for aluminum sheets (Fig. 16) for the sake of conciseness, as no significant difference was found between sheets and powder. The EDX spectrum (Fig. 16B) shows the presence of aluminum (Al), oxygen (O) and sodium (Na, shorter peak). This elemental composition suggests that the reaction produces compounds containing aluminum and oxygen, with a minor contribution from sodium. Moreover, the XRD pattern (Fig. 16C) exhibits several prominent peaks that align with both gibbsite (marked with orange squares) and bayerite (marked with black circles) reference patterns, thus highlighting the presence of both phases in the sample. Gibbsite and bayerite are two of known polymorphs of aluminum hydroxide ($Al(OH)_3$), with the former having a more stable crystal structure than the latter; the difference in formation energy is only 6–10 kJ mol^{-1} [14,27,60].

Subsequently, the average hydrogen production rate was calculated from the available dataset as a quantitative indicator of chemical kinetics, commonly employed in studies that involve hydrogen production from the reaction between aluminum and water [21,22]. Moreover, the specific production rate (i.e., hydrogen production rate normalized by the average mass of aluminum provided for reaction [37,42]) was also evaluated. The results for the tested configurations are included in Table 6.

Overall, the production rate found for the reaction between aluminum – both powder and sheets – and 5 M alkaline solution at 25 °C is consistent with the values reported in the open literature [33,37], powder granulometry being of the same order of magnitude. The same consideration holds for the production rate found for the reaction with 1 M solution at 50 °C [27,40], whereas no dataset appears available for comparison at higher values of molar concentration, arguably due to the rather fast kinetics in such conditions of temperature and alkaline solution concentration. On the other hand, the lack of studies at temperature below 0 °C makes the here proposed results an actual milestone in quantifying production rate under subzero conditions.

The obtained dataset of produced hydrogen allowed assessing the Arrhenius factor and activation energy as parameters instrumental in predicting reaction rate for the involved reaction. In the present evaluation, reaction rate could be calculated from the collected dataset through the concentration of hydrogen over time, then it was correlated with inverse temperature and the parameters of interest to quantify chemical kinetics by the Arrhenius equation [59,61]:

$$\ln(k) = \ln(A) + \left(\frac{E_a}{R}\right)\left(-\frac{1}{T}\right), \tag{7}$$

where k is reaction rate, A is a constant – the pre-exponential factor, also

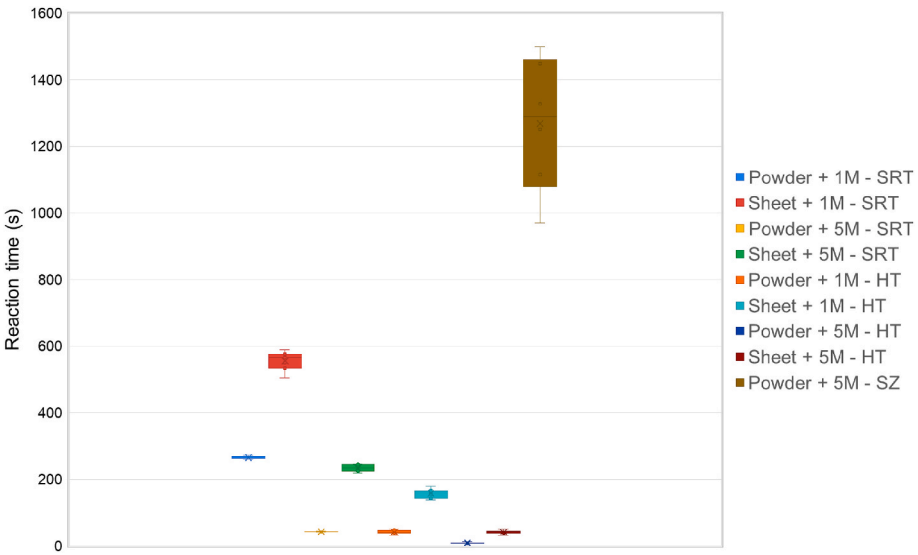

Fig. 15. Comparison between all the tested configurations in terms of reaction time through box plots (SZ: Subzero; SRT: Standard Reference Temperature, HT: Higher Temperature).

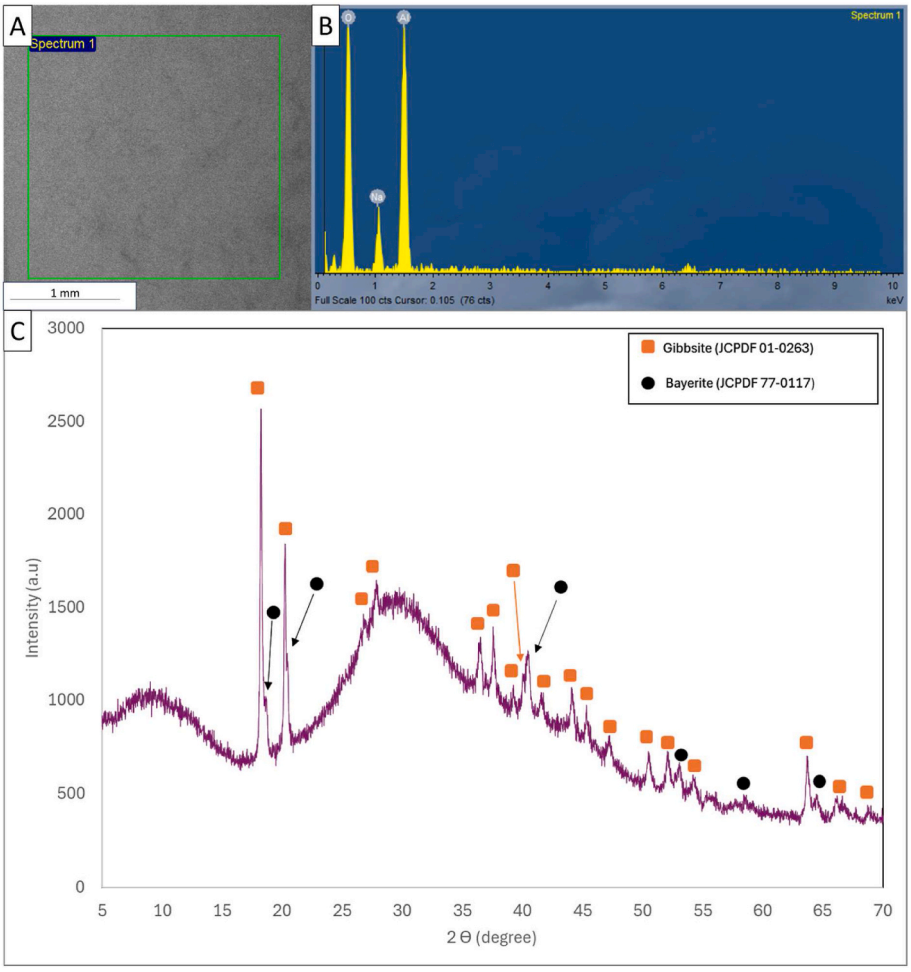

Fig. 16. Results from the analysis on anhydrous byproducts from the reaction involving aluminum sheets: (A) SEM image; (B) EDX spectra and (C) XRD pattern.

known as Arrhenius factor – that largely depends on the nature of the involved reactants, E_a is the molar activation energy for the reaction (i.e., the energy required to break the chemical bonds between the reacting molecules to generate products) and R is the universal gas constant. Fig. 17A shows a generic example of the Arrhenius plot, highlighting the relationship between temperature, activation energy and Arrhenius factor. On the other hand, the Arrhenius plot of Fig. 17B refers to the actual reaction rate for aluminum powder reacting with 5 M solution at

Table 6
Hydrogen production rate and specific production rate for the various tested configurations.

Nominal temperature (°C)	Degree of fragmentation (aluminum)	Molar concentration (alkaline solution)	H_2 production rate (mL min^{-1})	H_2 specific production rate (mL min^{-1} g^{-1})
−5	powder	5 M	5	80
25	powder	1 M	15	250
25	powder	5 M	100	1600
25	sheet	1 M	10	170
25	sheet	5 M	20	330
50	powder	1 M	110	1800
50	powder	5 M	380	6300
50	sheet	1 M	30	500
50	sheet	5 M	100	1600

the three selected temperature values (−5, 25 and 50 °C). A fitting trendline was then reconstructed by linear regression against the data points, which is expressed by Eq. (8):

$$y = (-6325.3 \pm 624.34)\, x + 20.526 \pm 2.1255. \quad (8)$$

The linear relationship between inverse temperature and natural logarithm of reaction rate constant is backed by a correlation coefficient R equal to −0.9952, which hints at strong correlation. To determine activation energy, the procedure described in Subsection 2.3 and in Fig. 5 was implemented: the slope of the trendline was multiplied by the universal gas constant (8.314 J K^{-1} mol^{-1}). The following equation presents the value of the slope, obtained from Eq. (8), and ultimately the calculated value of activation energy for the reaction between aluminum and NaOH/water solution:

$$\left|\frac{E_a}{R}\right| = 6325.3 \rightarrow E_a = 52 \text{ kJ mol}^{-1}. \quad (9)$$

The obtained result appears consistent with previous findings available in the open literature about activation energy for aluminum reaction with water, which lies in the 40–100 kJ mol^{-1} range [42–46]. As an additional outcome from reconstructing the trendline, its y-intercept yields the Arrhenius factor A, which resulted as equal to 20526 s^{-1}.

4. Conclusions

The present research was focused on hydrogen production through the exothermic reaction between aluminum (powder and sheets) and a NaOH/water solution (1 M and 5 M), at three different temperature conditions. Notably, this last parameter was varied between subzero – arguably an unprecedented effort in terms of temperature – and 50 °C, thus yielding a comprehensive range to evaluate chemical kinetics and addressing the potential use of such a hydrogen production method for mobile applications. For this purpose, an experiment was developed based on the Dietrich-Frühling method; an approach was also devised to reconstruct the amount of hydrogen generated over time from start through completion of the reaction.

As the first aspect, the effect of specific surface area on reaction kinetics, particularly emphasized when aluminum powder is used, appears to highlight the importance of surface morphology and degree of fragmentation in promoting chemical reactions. Furthermore, reactant concentration also impacts on reaction kinetics. The direct correlation between reactant concentration and reaction rate results from the significance of mass action in governing reaction dynamics, with higher concentration leading to more frequent collisions between molecules: passing from 1 M to 5 M alkaline concentration yielded faster completion, when keeping temperature constant. This study also identifies the critical effect of operating temperature on reaction kinetics: supplying additional kinetic energy to reacting particles by increasing temperature allows overcoming the activation energy barrier more quickly, thus promoting reaction rate, thereby highlighting the importance of temperature control in optimizing the conditions for achieving the desired amount of products or the desired production rate.

Interestingly, the effect of increasing a governing parameter (e.g., concentration) was proven effective in counterbalancing the decrease in another (e.g., temperature); for instance, aluminum powder reacting with 5 M alkaline solution at 25 °C featured almost the same reaction rate as aluminum powder reacting with 1 M alkaline solution or aluminum sheet reacting with 5 M alkaline solution at 50 °C. The classic theory of chemical reactions was finally employed to calculate activation energy (equal to about 50 kJ mol^{-1}) and Arrhenius coefficient (equal to 20526 s^{-1}) for the involved reaction between aluminum and NaOH/water solution. Overall, this work sheds light on the multifaceted interplay among surface area available for interaction between particles in a chemical reaction, reactant concentration and temperature in governing the kinetics of the involved reaction.

CRediT authorship contribution statement

Veronica Testa: Writing – original draft, Supervision, Resources, Methodology, Investigation, Formal analysis, Data curation, Conceptualization, Writing – review & editing. **Matteo Gerardi:** Investigation, Formal analysis, Data curation. **Luca Zannini:** Investigation, Formal analysis. **Marcello Romagnoli:** Supervision, Resources, Project administration, Methodology, Funding acquisition, Formal analysis, Conceptualization, Writing – review & editing. **Paolo E. Santangelo:** Writing – original draft, Supervision, Methodology, Investigation, Formal analysis, Data curation, Conceptualization, Writing – review &

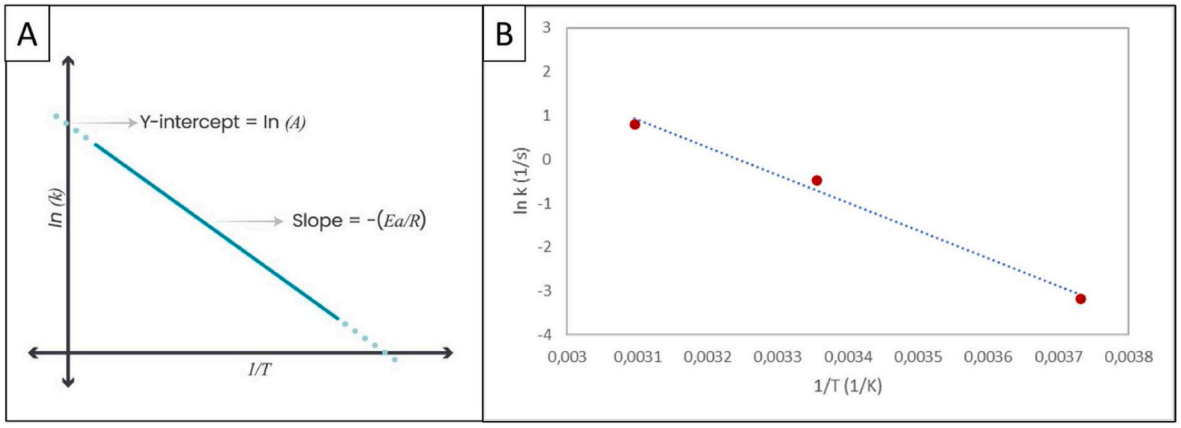

Fig. 17. Arrhenius plot: (A) generic diagram [39] and (B) plot obtained from the acquired dataset for the reaction between aluminum and NaOH/water solution.

editing.

Declaration of competing interest

The authors declare the following financial interests/personal relationships which may be considered as potential competing interests.

MUR – Ministero dell'Università e della Ricerca (The Italian ministry for higher education and research).

Acknowledgments

This project was funded under the National Recovery and Resilience Plan (NRRP), Mission 04, Component 2, Investment 1.5 – NextGenerationEU, ECS00000033, call for tender n. 3277 dated December 30, 2021, award number: 0001052 dated June 23, 2022. The authors wish to thank M.C. Rossi and C. Sgarlata (Università degli Studi di Modena e Reggio Emilia, Italy) for providing support to the chemical characterization of the samples.

References

[1] Nations U. World population prospects 2022. 2022.
[2] Tarhan C, Çil MA. A study on hydrogen, the clean energy of the future: hydrogen storage methods. J Energy Storage 2021;40:102676. https://doi.org/10.1016/j.est.2021.102676.
[3] Baykara SZ. Hydrogen: a brief overview on its sources, production and environmental impact. Int J Hydrogen Energy 2018;43:10605–14. https://doi.org/10.1016/j.ijhydene.2018.02.022.
[4] Balat M. Potential importance of hydrogen as a future solution to environmental and transportation problems. Int J Hydrogen Energy 2008;33:4013–29. https://doi.org/10.1016/J.IJHYDENE.2008.05.047.
[5] Abdin Z, Zafaranloo A, Rafiee A, Mérida W, Lipiński W, Khalilpour KR. Hydrogen as an energy vector. Renew Sustain Energy Rev 2020;120:109620. https://doi.org/10.1016/j.rser.2019.109620.
[6] Tang D, Tan G-L, Li G-W, Liang J-G, Ahmad SM, Bahadur A, et al. State-of-the-art hydrogen generation techniques and storage methods: a critical review. J Energy Storage 2023;64:152. https://doi.org/10.1016/j.est.2023.107196. 2352.
[7] Momirlan M, Veziroglu T. The properties of hydrogen as fuel tomorrow in sustainable energy system for a cleaner planet. Int J Hydrogen Energy 2005;30:795–802. https://doi.org/10.1016/j.ijhydene.2004.10.011.
[8] Sinigaglia T, Lewiski F, Santos Martins ME, Mairesse Siluk JC. Production, storage, fuel stations of hydrogen and its utilization in automotive applications-a review. Int J Hydrogen Energy 2017;42:24597–611. https://doi.org/10.1016/j.ijhydene.2017.08.063.
[9] Dawood F, Anda M, Shafiullah GM. Hydrogen production for energy: an overview. Int J Hydrogen Energy 2020;45:3847–69. https://doi.org/10.1016/J.IJHYDENE.2019.12.059.
[10] Møller KT, Jensen TR, Akiba E, wen Li H. Hydrogen - a sustainable energy carrier. Prog Nat Sci: Mater Int 2017;27:34–40. https://doi.org/10.1016/j.pnsc.2016.12.014.
[11] Ranjekar AM, Yadav GD. Steam reforming of methanol for hydrogen production: a critical analysis of catalysis, processes, and scope. Ind Eng Chem Res 2021;60:89–113. https://doi.org/10.1021/acs.iecr.0c05041.
[12] Nikolaidis P, Poullikkas A. A comparative overview of hydrogen production processes. Renew Sustain Energy Rev 2017;67:597–611. https://doi.org/10.1016/j.rser.2016.09.044.
[13] Levin DB, Pitt L, Love M. Biohydrogen production: prospects and limitations to practical application. Int J Hydrogen Energy 2004;29:173–85. https://doi.org/10.1016/S0360-3199(03)00094-6.
[14] Irankhah A, Seyed Fattahi SM, Salem M. Hydrogen generation using activated aluminum/water reaction. Int J Hydrogen Energy 2018;43:15739–48. https://doi.org/10.1016/j.ijhydene.2018.07.014.
[15] Wang HZ, Leung DYC, Leung MKH, Ni M. A review on hydrogen production using aluminum and aluminum alloys. Renew Sustain Energy Rev 2009;13:845–53. https://doi.org/10.1016/j.rser.2008.02.009.
[16] Kirton T, Saceleanu F, Salehi Mobarakeh M, Kholghy MR. Cogeneration of hydrogen, alumina, and heat from aluminum-water reactions. Int J Hydrogen Energy 2024;68:115–27. https://doi.org/10.1016/j.ijhydene.2024.04.038.
[17] Vishnevetsky I, Epstein M. Production of hydrogen from solar zinc in steam atmosphere. Int J Hydrogen Energy 2007;32:2791–802. https://doi.org/10.1016/j.ijhydene.2007.04.004.
[18] Uan J, Cho C, Liu K. Generation of hydrogen from magnesium alloy scraps catalyzed by platinum-coated titanium net in NaCl aqueous solution. Int J Hydrogen Energy 2007;32:2337–43. https://doi.org/10.1016/j.ijhydene.2007.03.014.
[19] Elitzur S, Rosenband V, Gany A. Study of hydrogen production and storage based on aluminum–water reaction. Int J Hydrogen Energy 2014;39:6328–34. https://doi.org/10.1016/j.ijhydene.2014.02.037.
[20] Smith IE. Hydrogen generation by means of the aluminum/water reaction. J Hydronautics 1972;6:106–9. https://doi.org/10.2514/3.48127.
[21] Huang X, Gao T, Pan X, Wei D, Lv C, Qin L, et al. A review: feasibility of hydrogen generation from the reaction between aluminum and water for fuel cell applications. J Power Sources 2013;229:133–40. https://doi.org/10.1016/j.jpowsour.2012.12.016.
[22] Bolt A, Dincer I, Agelin-Chaab M. A review of unique aluminum-water based hydrogen production options. Energy Fuel 2021;35:1024–40. https://doi.org/10.1021/ACS.ENERGYFUELS.0C03674/ASSET/IMAGES/MEDIUM/EF0C03674_0015.GIF.
[23] Shmelev V, Nikolaev V, Lee JH, Yim C. Hydrogen production by reaction of aluminum with water. Int J Hydrogen Energy 2016;41:16664–73. https://doi.org/10.1016/j.ijhydene.2016.05.159.
[24] Hiraki T, Takeuchi M, Hisa M, Akiyama T. Hydrogen production from waste aluminum at different temperatures, with LCA. Mater Trans 2005;46:1052–7. https://doi.org/10.2320/matertrans.46.1052.
[25] Pedicini R, Romagnoli M, Santangelo PE. A critical review of polymer electrolyte membrane fuel cell systems for automotive applications: components, materials, and comparative assessment. Energies 2023;16:3111. https://doi.org/10.3390/en16073111.
[26] Schlapbach L, Züttel A. Hydrogen-storage materials for mobile applications. Nature 2001;414:353–8. https://doi.org/10.1038/35104634.
[27] Porciúncula CB, Marcilio NR, Tessaro IC, Gerchmann M. Production of hydrogen in the reaction between aluminum and water in the presence of NaOH and KOH. Braz J Chem Eng 2012;29:337–48. https://doi.org/10.1590/S0104-66322012000200014.
[28] Czech E, Troczynski T. Hydrogen generation through massive corrosion of deformed aluminum in water. Int J Hydrogen Energy 2010;35:1029–37. https://doi.org/10.1016/j.ijhydene.2009.11.085.
[29] Uehara K, Takeshita H, Kotaka H. Hydrogen gas generation in the wet cutting of aluminum and its alloys. J Mater Process Technol 2002;127:174–7. https://doi.org/10.1016/S0924-0136(02)00121-8.
[30] Fan MQ, Xu F, Sun LX. Studies on hydrogen generation characteristics of hydrolysis of the ball milling Al-based materials in pure water. Int J Hydrogen Energy 2007;32:2809–15. https://doi.org/10.1016/J.IJHYDENE.2006.12.020.
[31] Soler L, Macanás J, Muñoz M, Casado J. Aluminum and aluminum alloys as sources of hydrogen for fuel cell applications. J Power Sources 2007;169:144–9. https://doi.org/10.1016/J.JPOWSOUR.2007.01.080.
[32] Martínez SS, Benítes WL, Gallegos AAÁ, Sebastián PJ. Recycling of aluminum to produce green energy. Sol Energy Mater Sol Cell 2005;88:237–43. https://doi.org/10.1016/J.SOLMAT.2004.09.022.
[33] Ma GL, Dai H Bin, Zhuang DW, Xia HJ, Wang P. Controlled hydrogen generation by reaction of aluminum/sodium hydroxide/sodium stannate solid mixture with water. Int J Hydrogen Energy 2012;37:5811–6. https://doi.org/10.1016/J.IJHYDENE.2011.12.157.
[34] Ho CY, Huang CH. Enhancement of hydrogen generation using waste aluminum cans hydrolysis in low alkaline de-ionized water. Int J Hydrogen Energy 2016;41:3741–7. https://doi.org/10.1016/J.IJHYDENE.2015.11.083.
[35] Rendón MV, Calderón JA, Fernández P. Evaluation of the corrosion behavior of the al-356 alloy in NaCl solutions. Quim Nova 2011;34:1163–6. https://doi.org/10.1590/S0100-40422011000700011.
[36] Bolt A, Dincer I, Agelin-Chaab M. Experimental study of hydrogen production process with aluminum and water. Int J Hydrogen Energy 2020;45:14232–44. https://doi.org/10.1016/j.ijhydene.2020.03.160.
[37] Aleksandrov YA, Tsyganova EI, Pisarev AL. Reaction of aluminum with dilute aqueous NaOH solutions. Russ J Gen Chem 2003;73:689–94. https://doi.org/10.1023/A:1026114331597.
[38] Jung CR, Kundu A, Ku B, Gil JH, Lee HR, Jang JH. Hydrogen from aluminium in a flow reactor for fuel cell applications. J Power Sources 2008;175:490–4. https://doi.org/10.1016/J.JPOWSOUR.2007.09.064.
[39] Soler L, Candela AM, Macanás J, Muñoz M, Casado J. Hydrogen generation by aluminum corrosion in seawater promoted by suspensions of aluminum hydroxide. Int J Hydrogen Energy 2009;34:8511–8. https://doi.org/10.1016/J.IJHYDENE.2009.08.008.
[40] Soler L, Candela AM, Macanás J, Muñoz M, Casado J. In situ generation of hydrogen from water by aluminum corrosion in solutions of sodium aluminate. J Power Sources 2009;192:21–6. https://doi.org/10.1016/J.JPOWSOUR.2008.11.009.
[41] Soler L, Candela AM, Macanás J, Muñoz M, Casado J. Hydrogen generation from water and aluminum promoted by sodium stannate. Int J Hydrogen Energy 2010;35:1038–48. https://doi.org/10.1016/J.IJHYDENE.2009.11.065.
[42] Yavor Y, Goroshin S, Bergthorson JM, Frost DL, Stowe R, Ringuette S. Enhanced hydrogen generation from aluminum-water reactions. Int J Hydrogen Energy 2013;38:14992–5002. https://doi.org/10.1016/j.ijhydene.2013.09.070.
[43] Gai W-Z, Liu W-H, Deng Z-Y, Zhou J-G. Reaction of Al powder with water for hydrogen generation under ambient condition. Int J Hydrogen Energy 2012;37:13132–40. https://doi.org/10.1016/j.ijhydene.2012.04.025.
[44] A.P. Lyashko; A.A. Medvinskii; G.G. Savel'ev. Specific features of the interaction of submicron aluminum powders with liquid water: macrokinetics, products, and manifestation of self-heating. Kinet Catal.;31:967–972. .
[45] Studart AR, Innocentini MDM, Oliveira IR, Pandolfelli VC. Reaction of aluminum powder with water in cement-containing refractory castables. J Eur Ceram Soc 2005;25:3135–43. https://doi.org/10.1016/J.JEURCERAMSOC.2004.07.004.
[46] Rosenband V, Gany A. Application of activated aluminum powder for generation of hydrogen from water. Int J Hydrogen Energy 2010;35:10898–904. https://doi.org/10.1016/J.IJHYDENE.2010.07.019.

[47] Liu M, Liu H, Chen K, Sun J, Wang H, Liu J, et al. An Al–Li alloy/water system for superior and low-temperature hydrogen production. Inorg Chem Front 2021;8:3473–81. https://doi.org/10.1039/D1QI00487E.
[48] Forni F, Degruyter W, Bachmann O, De Astis G, Mollo S. Long-term magmatic evolution reveals the beginning of a new caldera cycle at Campi Flegrei. Sci Adv 2018;4. https://doi.org/10.1126/sciadv.aat9401.
[49] De Astis G, Peccerillo A, Kempton PD, La Volpe L, Wu TW. Transition from calc-alkaline to potassium-rich magmatism in subduction environments: geochemical and Sr, Nd, Pb isotopic constraints from the island of Vulcano (Aeolian arc). Contrib Mineral Petrol 2000;139:684–703. https://doi.org/10.1007/s004100000172.
[50] Barbieri L, Bigi A, Andreola F, Lancelotti I, Ghermandi G, Teresa Cotes Palomino M, et al. Environmental impact estimation of ceramic lightweight aggregates production starting from residues. Int J Appl Ceram Technol 2021;18:353–68. https://doi.org/10.1111/ijac.13665.
[51] Kaye GWC, Laby TH. Tables of physical and chemical constants and some mathematical functions. 1921. https://doi.org/10.1021/j150376a021.
[52] Helrich CS. Modern thermodynamics with statistical mechanics. Berlin, Heidelberg: Springer Berlin Heidelberg; 2009. https://doi.org/10.1007/978-3-540-85418-0.
[53] Shapiro SS, Wilk MB. An analysis of variance test for normality (complete samples). Biometrika 1965;52:591. https://doi.org/10.2307/2333709.
[54] Kim H-Y. Analysis of variance (ANOVA) comparing means of more than two groups. Restor Dent Endod 2014;39:74. https://doi.org/10.5395/rde.2014.39.1.74.
[55] Andy Field, Field Zoe, Miles Jeremy. Discovering statistics using R. 2012.
[56] Pardo S. Statistical analysis of empirical data. Cham: Springer International Publishing; 2020. https://doi.org/10.1007/978-3-030-43328-4.
[57] Hammer Ø, Harper DAT, Ryan PD. PAST: paleontological statistics software package for education and data analysis. Palaeontologia Electronica. Palaeontol Electron 2001;4.
[58] Wang X, Li G, Eckhoff RK. Kinetics study of hydration reaction between aluminum powder and water based on an improved multi-stage shrinking core model. Int J Hydrogen Energy 2021;46:33635–55. https://doi.org/10.1016/J.IJHYDENE.2021.07.191.
[59] Silberberg M, Amateis P. Chemistry: the molecular nature of matter and change. 2000.
[60] Digne M, Sautet P, Raybaud P, Toulhoat H, Artacho E. Structure and stability of aluminum hydroxides: a theoretical study. J Phys Chem B 2002;106:5155–62. https://doi.org/10.1021/jp014182a.
[61] Wang J, Wan W. Kinetic models for fermentative hydrogen production: a review. Int J Hydrogen Energy 2009;34:3313–23. https://doi.org/10.1016/J.IJHYDENE.2009.02.031.